Available online at www.sciencedirect.com
SCIENCE DIRECT
ELSEVIER
Deep-Sea Research I 53 (2006) 608–626
DEEP-SEA RESEARCH PART I
www.elsevier.com/locate/dsr

Interannual variability of the Atlantic water layer in the West Spitsbergen Current at 76.5°N in summer 1991–2003

Pawel Schlichtholz*, Ilona Goszczko

Institute of Oceanology PAS, Powstancow Warszawy 55, 81-712 Sopot, Poland

Received 21 February 2005; received in revised form 2 January 2006; accepted 7 January 2006
Available online 3 March 2006

Abstract

The Atlantic water (AW) layer in the West Spitsbergen Current (WSC) is an important source of heat and salt for the Arctic Ocean and the areas of deep convection in the Greenland Sea. In the southern Fram Strait, the WSC has two main branches, an eastern core on the continental slope and a western one in the Knipovich Ridge area. Here we analyze interannual variability of the heat content and geostrophic flow (level of no motion at 1000 m) in the AW layer (temperature above 2 °C and salinity above 34.9) in both branches of the WSC using summer hydrographic data along a zonal section from 6° to 15°E at 76.5°N occupied by R/V *Oceania* from 1996 to 2003. In the eastern branch, our time series go back to 1991. In particular, we make inferences of correlation with the winter North Atlantic Oscillation (NAO) index. The AW temperature series in the eastern core show two warm periods, one at the beginning of the 1990s and one at the beginning of the 2000s, separated by a cold event in 1997–1998. There is a competition between a lagged and non-lagged response to the NAO. While the cold event lags the spectacular drop of the NAO index in 1996, the temperature extremes in the warm periods are concomitant with the extremes of the NAO index in these periods. However, if we consider the average thickness of the AW layer on the whole section in the 1996–2003 period, we obtain a high correlation ($r = 0.94$) in which the NAO index leads by 1 yr. In contrast, the geostrophic flow shows a close relation to the NAO only in limited areas. The most striking result is a nearly perfect correlation for the strength of the western branch of the WSC, which evolves without a lag and in opposite phase to the NAO index ($r = -0.96$). Possible causes of links between the evolution of the AW layer and the NAO are discussed based on information available from the literature. It is suggested that both the eastern and western branches undergo interannual variations which are coherent from the northern North Atlantic to Fram Strait. A conclusion is drawn that the summer AW thickness in the eastern branch may be a proxy for the annual mean volume transport in the WSC.

Keywords: West Spitsbergen Current; Atlantic water; Heat content; Geostrophic flow; Temporal variations; Climate

1. Introduction

The West Spitsbergen Current (WSC), which flows northward on the eastern side of Fram Strait (Fig. 1a), injects warm and saline Atlantic water (AW) below the ice-covered, cold and fresh Polar water (PW) cap of the Arctic Ocean (e.g., Aagaard

*Corresponding author. Tel.: +48 58 5517283; fax: +48 58 5512130.
E-mail address: schlicht@ocean.iopan.gda.pl (P. Schlichtholz).

0967-0637/$ - see front matter © 2006 Elsevier Ltd. All rights reserved.
doi:10.1016/j.dsr.2006.01.001

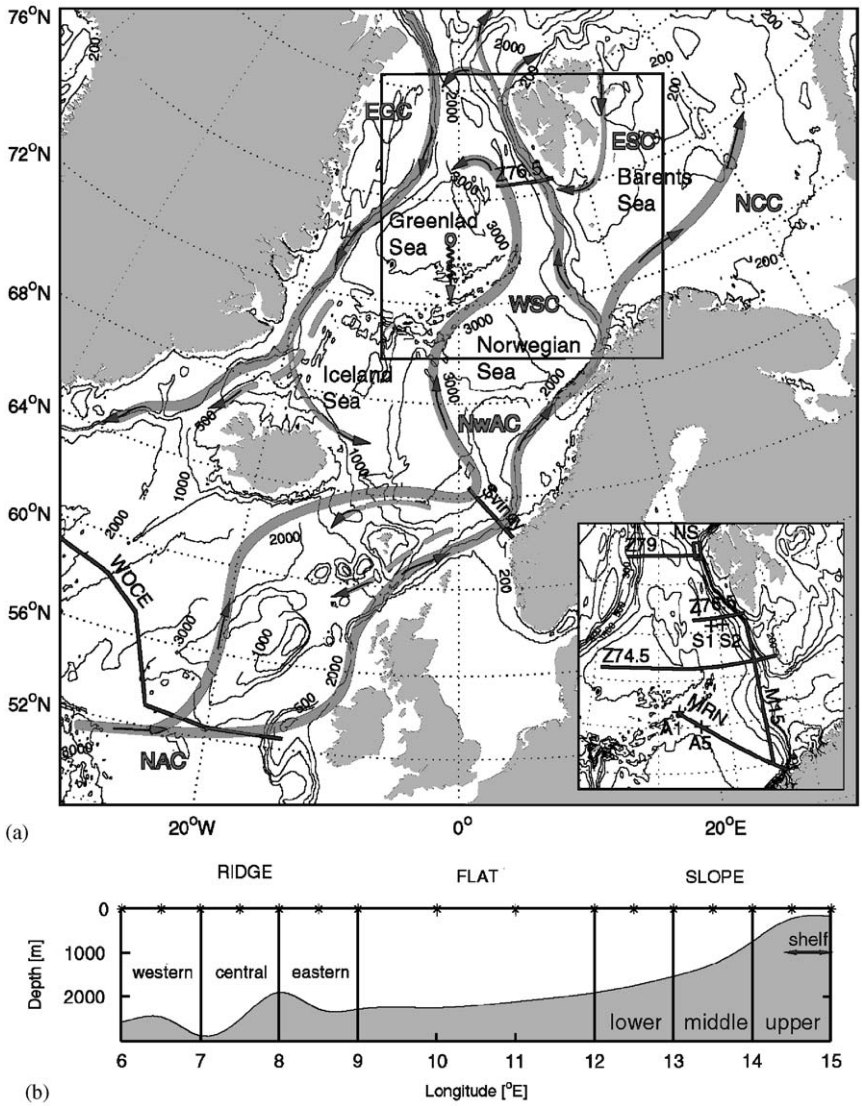

Fig. 1. Area of interest: (a) Bottom depth (m) and schematics of main currents: NAC—North Atlantic Current, NwAC—Norwegian Atlantic Current, NCC—North Cape Current, WSC—West Spitsbergen Current, ESC—East Spitsbergen Current, and EGC—East Greenland Current. The zonal line across the WSC at 76.5°N indicates the position of the main hydrographic section analyzed in the present study. The line across the NwAC (NAC) is the Svinøy (WOCE) section referred to in the text. The section at 76.5°N (Z76.5) is re-plotted in the inlet which also shows some other sections. MRN (M15) is a Mohns Ridge-Norway (15°E) section occupied by R/V *Oceania* in 2000–2003 (1991–1999). Stations A1 and A5 indicate limits of the Mohns Ridge slope. The box NS (points S1 and S2) shows a northern slope area (two stations on the Sørkapp section) for temperature evolution comparisons. The zonal line Z79 (Z74.5) indicates a current meter (hydrographic) section for transport estimate comparisons; (b) bottom topography along the 76.5°N section and its division into the (upper, middle and lower) SLOPE, FLAT and (western, central and eastern) RIDGE areas. The stars indicate typical locations of the hydrographic stations in 1996–2003.

et al., 1985). While the southward flowing East Greenland Current (EGC) is an important source of fresh water for the North Atlantic, the WSC is an important source of heat for the Arctic Ocean (e.g., Simonsen and Haugan, 1996). AW is supplied to the Nordic Seas across the Greenland–Scotland Ridge (GSR) by the North Atlantic Current. There are two major pathways by which AW gets to Fram Strait. The eastern branch of the Norwegian Atlantic Current (NwAC) is a shelf edge current which bifurcates northwest of Norway into a Fram Strait stream and a stream carrying AW towards the Arctic Ocean via the Barents Sea. The western branch is a topographically guided jet in the

transition zone between AW and Arctic waters in the Nordic Seas (Orvik and Niiler, 2002; Jakobsen et al., 2003). Since some AW recirculates in Fram Strait (e.g., Gascard et al., 1995; Schlichtholz and Houssais, 1999b), the current is also a major source of heat (and salt) for the areas of intermediate and deep convection in the Greenland Sea (e.g., Gascard et al., 2002), which feeds the deep branch of the meridional overturning circulation (e.g., Mauritzen, 1996).

A number of studies have shown that properties of AW in the WSC undergo considerable interannual and longer term variability reflecting contemporary climate fluctuations (Swift et al., 1997; Blindheim et al., 2000; Dickson et al., 2000; Saloranta and Haugan, 2001). All these studies linked variations in the AW hydrography to variations in large-scale atmospheric patterns. In particular, correlations with the winter North Atlantic Oscillation (NAO) index were estimated. However, analyses were based on data from limited areas. The time-dependence in the two branches of the WSC has not been investigated simultaneously. In fact, the variability in the western branch has not been studied at all.

In a recent study (Schlichtholz and Goszczko, 2005), we analyzed variability in the AW properties on a meridional section south of Fram Strait (M15 in Fig. 1a). We concluded that there was a time lag between the AW temperature and salinity in the 1990s. Here we focus on variability in the summer heat content, geostrophic flow, and associated variables of the AW layer in the southeastern Fram Strait and its relation to the winter NAO index. For this purpose we use the longest from hydrographic series acquired in the Nordic Seas by the Institute of Oceanology in Sopot, i.e., a repeated zonal section at 76.5°N (Z76.5 in Fig. 1a). Our series, although not as long as some other series, allow us not only to study the most recent (1991–2003) variability in the main core of the WSC, but also to investigate the cross slope structure of the variability in a period (1996–2003) in which a recovery from particularly cold to particularly warm conditions occurred. In addition, recent (summer 2000–2003) hydrographic data from a section between the Mohns Ridge and Norway (MRN in Fig. 1a) will be used as supportive material.

2. Hydrographic data

The Institute of Oceanology in Sopot has acquired hydrographic data in the main paths of AW from the North Atlantic to the Arctic Ocean for several years during summer cruises of R/V *Oceania* (e.g., Schlichtholz and Jankowski, 1993; Piechura et al., 2002; Schlichtholz and Goszczko, 2005). Here we use observations made, typically in July, every year from 1991 to 2003 along a zonal hydrographic section at 76.5°N (Fig. 1). From 1991 to 1995, the 76.5°N section covered a variable portion of the continental slope, with a typical spacing between stations of 1° of longitude. Since then the section has been extended farther westward and typically sampled every 0.5° of longitude in the SLOPE area (12°–15°E) and in the area of the mid-ocean (Knipovich) ridge (6°–9°E), hereafter referred to as the RIDGE area. In the central, nearly flat bottom area between the RIDGE and the SLOPE, hereafter referred to as the FLAT area, the resolution was 1° of longitude. The SLOPE area is divided into three parts (Fig. 1b). On the middle SLOPE (750–1500 m isobaths), there are data for the entire 1991–2003 period. On the lower SLOPE (1500–1900 m isobaths) and on the upper SLOPE (200–750 m isobaths), the time series span the 1995–2003 period. The RIDGE area is divided into a western, central and eastern part. The western RIDGE area is centered at a height which is ~2500 m deep. The central RIDGE area is characterized by a considerable bottom slope. It extends from the rift valley, deeper than 3000 m, to the shallowest point on the ridge which has a relative height of more than 1000 m. The eastern RIDGE area covers the eastern slope of the ridge descending to ~2300 m depth.

The hydrographic measurements were made with conductivity-temperature-depth (CTD) Guildline 8770 instruments in 1991 and 1992 and CTD Sea-Bird 9/11 instruments afterwards. The soundings were made down to at least the 1000 db level or the bottom if shallower. Recordings were preprocessed and 5 db averages of potential temperature (θ), salinity (S) and corresponding potential density (σ_θ) were constructed. The geostrophic velocity derived at the mid-station locations was referenced to the 1000 db level (or the bottom if shallower). A zero reference velocity was assumed. MATLAB routines were used for standard calculations (Morgan, 1994). The vertical shear was linearly extrapolated below the shallower level of each pair of adjacent stations from the average value in a 20 m layer above the shallower level to zero at the bottom. The assumption of a zero reference velocity misses a depth-independent flow, which may significantly

contribute to the transport on the SLOPE as indicated by current measurements along a zonal section at 79°N (Z79 in Fig. 1a) reported by Fahrbach et al. (2001) and Schauer et al. (2004). On the other hand, the assumption of a zero velocity at the 1000 db level may be more or less justified in the RIDGE area. This is suggested by a reversal of the flow direction seen in the current meter section (Fahrbach et al., 2001, Fig. 4) or a geostrophic velocity section at 77.6°N obtained form the MIZEX 84 hydrographic data using an inverse model (Schlichtholz and Houssais, 1999a, Fig. 11).

To obtain time-mean distributions in the 1996–2003 period, data in each year were first horizontally interpolated onto a common equidistant grid with limits at 6°E and 15°E. For variables between 14.5° and 15°E in 1999, we have assumed constant values, equal to the data from the easternmost station (14.75°E) in this year. Parameters involving vertical integration such as the AW layer thickness (D_{AW}), average temperature (θ_{AW}), heat content (H_{AW}), net geostrophic transport (V_{AW}), and the associated heat flux (F_{AW}) were directly estimated from the hydrographic data. Then, they were interpolated onto the common grid before further processing, e.g., calculation of averages in a part or for the entire (WHOLE) section. The temperature reference for the calculations of H_{AW} and F_{AW} was 0 °C.

The hydrographic data along the MRN section (18 stations each summer of the 2000–2003 period) were processed in a similar way. A detailed analysis of this section will be presented elsewhere. Here we will only discuss D_{AW} averaged over the entire section and V_{AW} averaged over its westernmost part, between stations A1 and A5 (Fig. 1a). The stations lie on the Norwegian Sea side of the Mohns Ridge over the bottom sloping from the depth of 1800 m at A1 to 2900 m at A5 (the deepest station on the section).

3. Hydrographic structure across the West Spitsbergen Current

3.1. Mean distributions

In the mean distributions of θ and S in the 1996–2003 period, the eastern branch of the WSC can be recognized as a warm and saline core on the middle SLOPE (Fig. 2). For further references, here we adopt a common definition of AW, i.e., $\theta > 2$ °C and $S > 34.9$ (e.g., Aagaard et al., 1985; Schlichtholz and Houssais, 2002). A front at the shelf break separates the AW core from cold and fresh waters of Arctic origin, presumably supplied by the East Spitsbergen Current (Fig. 1a). The front must be a continuation of the Polar Front in the Barents Sea into Fram Strait (e.g., Saloranta and Svendsen, 2001).

A frontal structure, which has a particularly strong signature in σ_θ below a 50 m surface layer (Fig. 3a), also appears immediately west of the core. This structure, hereafter referred to as the Slope Front, is associated with the eastern kernel of the northward geostrophic flow (Fig. 3b). The kernel is localized between 13° and 13.5°E where the mean surface velocity exceeds 16 cm s^{-1}. On the eastern side of the AW core, the thermal stratification below the surface layer results in the southward direction of the geostrophic velocity. In spite of stronger gradients across the Polar Front than across the Slope Front, the southward flow has a smaller magnitude (up to 7 cm s^{-1}) than the northward flow because of a shallow water column on the shelf.

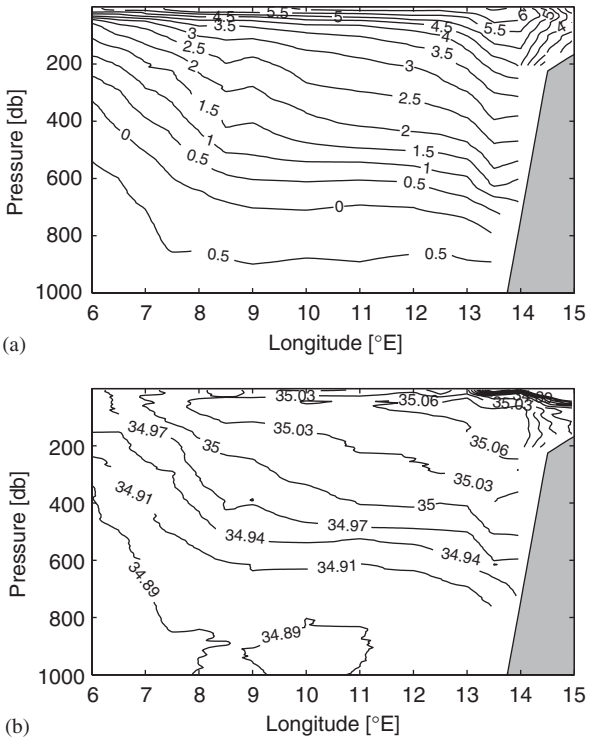

Fig. 2. Vertical distribution of mean water properties in the 1996–2003 period: (a) Potential temperature (°C); (b) salinity. In (b), in addition to isohalines plotted every 0.03, the isohaline of 34.89 is added.

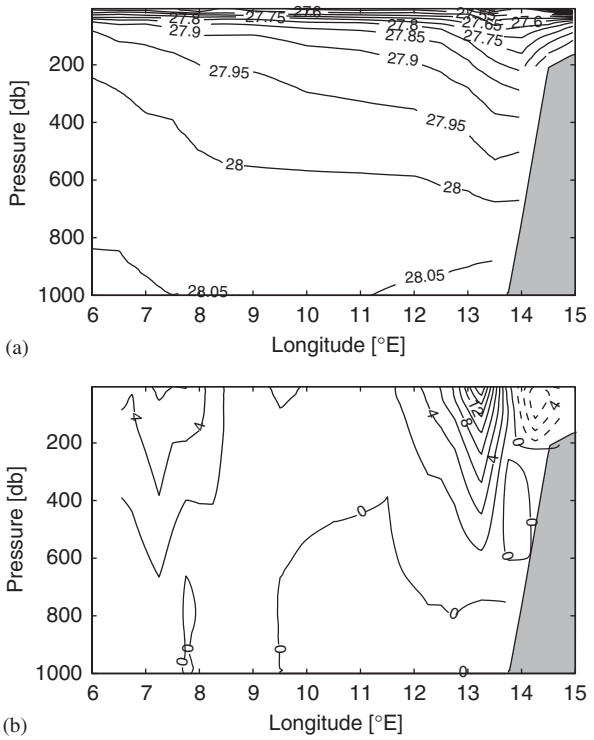

Fig. 3. Same as Fig. 2 but for other variables: (a) Potential density (σ_θ); (b) geostrophic velocity (cm s^{-1}) referenced to the 1000 db level or the bottom if shallower. Positive (negative) values indicate northward (southward) flow.

Strong horizontal temperature and salinity gradients below the surface layer also appear in the RIDGE area (Fig. 2). They are a manifestation of another part of the regional frontal system which separates AW from cold and fresh Arctic waters of the Greenland gyre (van Aken and Budéus, 1995). The density gradients associated with this Arctic Front (Fig. 3a) indicate the presence of a western branch of the WSC. The western kernel is localized over the steep slope of the central RIDGE area where the mean surface velocity exceeds 6 cm s^{-1} (Fig. 3b).

The mean net geostrophic transport in the total 0–1000 db layer (V_t) is compared to the corresponding transport in the AW layer in Table 1 where also statistics of other AW variables are given. The overall V_{AW} of 1.5 Sv (1 Sv = 10^6 m^3 s^{-1}) results from a northward transport of 2.2 Sv and a southward transport of 0.7 Sv. The corresponding V_t is larger only by 0.6 Sv. The SLOPE, RIDGE and FLAT areas contribute to the overall V_{AW} 0.8, 0.4, and 0.3 Sv, respectively. The overall net heat flux in the AW layer of 22.5 TW (36.6 TW northward and 14.1 TW southward) is distributed between the areas practically in the same proportions since θ_{AW} varies little along the section.

Table 1
Statistics (mean ± 1 standard deviation) of the total net geostrophic transport (V_t) in the 0–1000 db layer and AW variables (see Section 2 for explanation of symbols) in different parts of the 76.5°N section for the 1996–2003 period. The superscript (+) indicates the northward contribution to the net transport

Variable	SLOPE	RIDGE	FLAT	WHOLE
V_t (Sv)	0.8 ± 0.7	1.0 ± 0.9	0.3 ± 1.0	2.1 ± 0.9
V_{AW} (Sv)	0.8 ± 0.6	0.4 ± 0.5	0.3 ± 0.7	1.5 ± 0.7
$V_{AW}^{(+)}$ (Sv)	1.2 ± 0.4	0.6 ± 0.4	0.4 ± 0.6	2.2 ± 0.8
F_{AW} (TW)	12.8 ± 10.3	5.6 ± 6.1	4.1 ± 10.2	22.5 ± 11.5
$F_{AW}^{(+)}$ (TW)	21.9 ± 8.6	7.5 ± 4.8	7.2 ± 8.7	36.6 ± 13.9
θ_{AW} (°C)	3.7 ± 0.4	3.2 ± 0.4	3.2 ± 0.4	3.4 ± 0.4
D_{AW} (m)	395 ± 85	215 ± 55	380 ± 95	330 ± 65
H_{AW} (GJ m^{-2})	6.1 ± 1.7	2.8 ± 0.8	5.0 ± 1.4	4.6 ± 1.2

3.2. Distributions in particular years

The two branches of the WSC change their properties and relative strength. They also move laterally and sometimes the two-branch structure is even lost. An illustration is provided in Fig. 4 which shows the temperature distribution for two particular years, 1997 and 2000. In 1997, the upper ocean was generally much cooler than the mean state. The negative anomaly was extreme (−4 °C) in a near surface (50–100 m) layer at both limits of the section (Fig. 5a). In contrast, in 2000, nearly the whole section was much warmer than the mean state. A strong warm anomaly (2 °C) appeared in the core on the SLOPE, and also in a core localized as far west as 7°E (Fig. 5b).

In both, 1997 and 2000 anomalies of the opposite sign to the overall tendencies in these years (warm in 1997 and cold in 2000) appeared around the 400 m level in the central/eastern RIDGE area (Fig. 5). The positive anomaly (1.1 °C) in 1997 was a result of a westward extension of the quasi-horizontal run of the isotherms in the FLAT area into the area where the isotherms tilt up in the mean (Fig. 2a). As a consequence, 1997 was a year with a sharp Arctic Front and the most clear division of the WSC into two branches (Fig. 6a). The western kernel (a maximum of 16 cm s^{-1}) was nearly as strong as the eastern kernel (a maximum of 19 cm s^{-1}). The latter was shifted by half a degree toward the shelf compared to the mean flow.

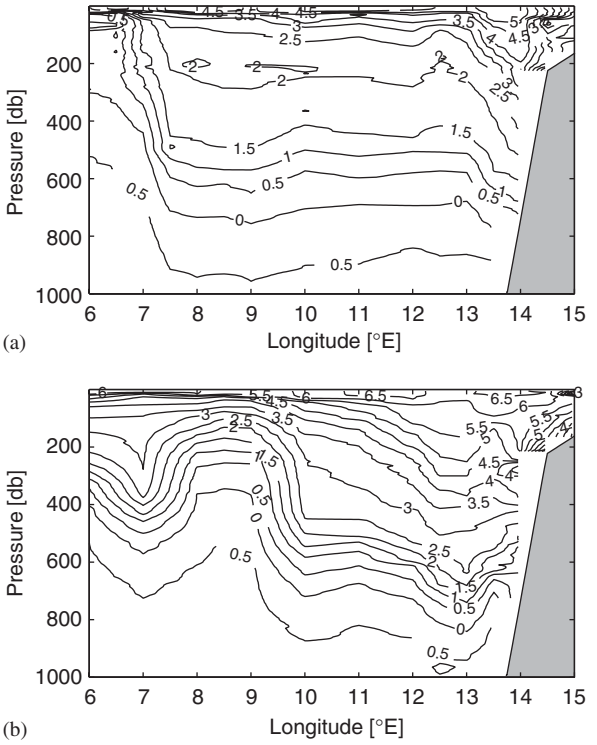

Fig. 4. Vertical distribution of potential temperature (°C) along the 76.5°N section in particular years: (a) 1997; (b) 2000.

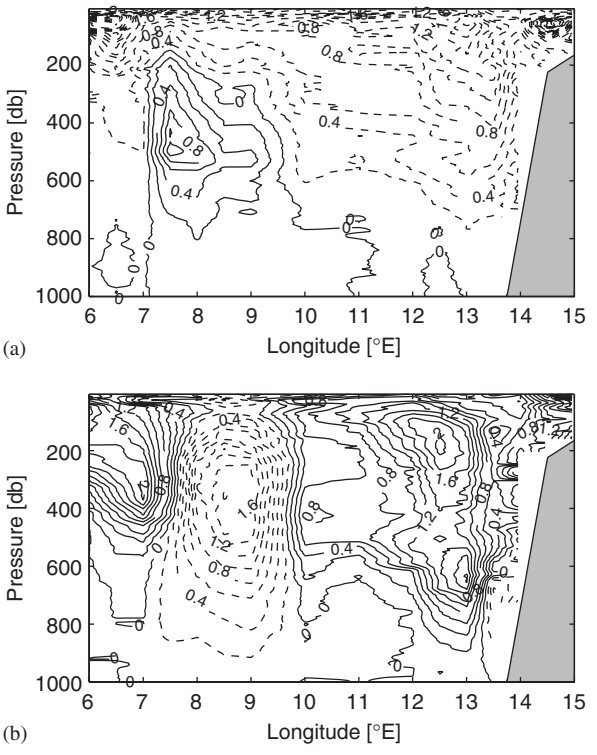

Fig. 5. Same as Fig. 4 but for potential temperature anomaly (°C) with respect to the mean in the 1996–2003 period.

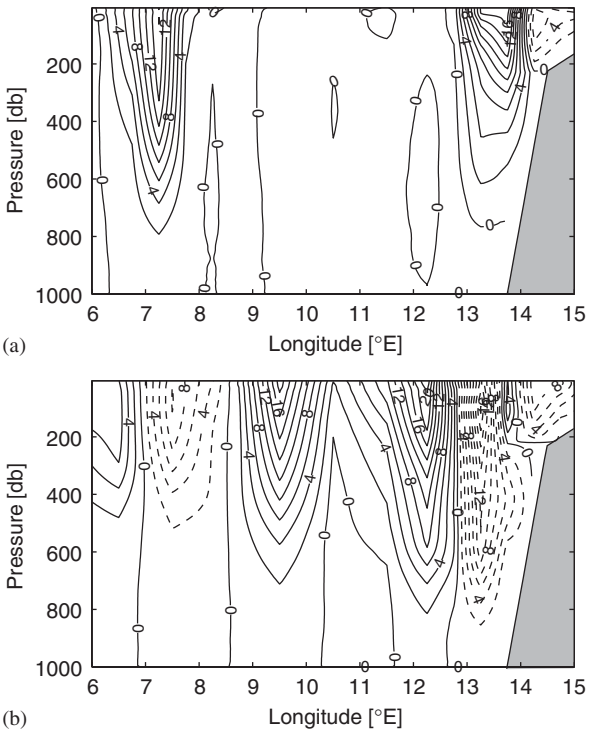

Fig. 6. Same as Fig. 4 but for geostrophic velocity (cm s^{-1}). Sign convention is the same as in Fig. 3b.

The negative anomaly (−1.8 °C) in 2000 was associated with an intrusion of cold water in the eastern RIDGE area (Fig. 4b). The local doming of the isotherms in this area together with the deepening of the isotherms at 7°E may be a manifestation of baroclinic instability, which is known to occur often in the Arctic Front (van Aken and Budéus, 1995). Eddies or meanders are frequent in Fram Strait as shown by the current meter measurements (Schauer et al., 2004) or drifter data (Gascard et al., 1995). They are thought to be essential for the recirculation of AW towards the EGC. In our 2000 section, an imprint of meso-scale processes is clearly seen on the SLOPE where the warm core was split into two sub-cores. This may be a result of breaking of topographic waves, which are known to significantly contribute to short-term current fluctuations along the continental slope in the NwAC (Skagseth and Orvik, 2002). Only a remnant of a typical eastern branch (a maximum of 5 cm s^{-1}) appeared at the location of the 1997 kernel (Fig. 6b). The strongest northward flow (maxima of ~20 cm s^{-1}) was located on the lower SLOPE and in the FLAT area.

3.3. 'Anatomy' of the AW layer

The presence of a more or less pronounced warm and saline core on the SLOPE is permanent as displayed by the sequence of distributions of D_{AW} from 1996 to 2003 (Fig. 7a and b). The location of the maximum thickness shows that the core migrated in this period from a station at the 750 m isobath to a station at the 1500 m isobath. The easternmost position of the core (14°E) was also its most frequent position while its migration to the westernmost position (13°E) was a single event, which occurred in 2000. In spite of lateral movements of the core in some years and a variable thickness, ranging from 400 to 700 m, the most significant eastward drop of D_{AW} (by 300–500 m) always occurred in the Polar Front on the upper SLOPE.

The AW layer in the WSC is often viewed as a wedge hanging on the shelf break and gradually thinning westward. This is a zero-order description, valid for mean distributions of water properties. In all snapshots at 76.5°N, D_{AW} shows a secondary, western maximum on the eastern side of the Arctic Front (Figs. 7a and b). Since the location of the western core is highly variable, the core is smeared out in the mean (Fig. 7c). The western core may be as thick as 500 m, as was the case in 1996, and in 2001 when it was even thicker than the eastern core. However, the area of the most frequent appearance of the western core, the eastern RIDGE area, is characterized by variations of D_{AW} within a range (400 m) larger than in the eastern core.

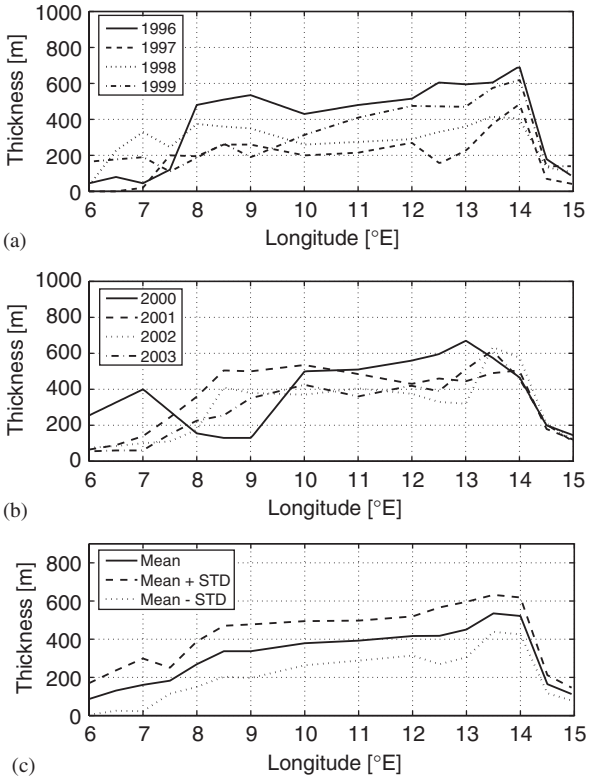

Fig. 7. Distribution of the AW thickness (m) along the 76.5°N section: (a) Years 1996–1999; (b) years 2000–2003; (c) mean and mean ±1 standard deviation in the 1996–2003 period.

A large variability also appears on the lower SLOPE since the Slope Front is often, but not always found immediately west of the eastern AW core (Figs. 7a and b). A smaller variability in the core than west of it has already been noted by Saloranta and Haugan (2001) in the context of long-term trends. The core is clearly recognized by a minimum of relative variability in D_{AW}. While the standard deviation (STD) in the 1996–2003 period attains (exceeds) 30% of the mean D_{AW} on the shelf (lower SLOPE), it does not reach 20% of the mean in the core area (Fig. 7c). A relatively low variability is also characteristic for a narrow band of the Arctic Front in the central RIDGE area. At 7.5°E, the STD is less than 40% of the mean D_{AW}, while it exceeds 40% of the mean in the eastern RIDGE area and jumps to more than 80% of the mean in the western RIDGE area. The absolute value of the STD at 7.5°E (70 m) is even lower than its value in the AW core on the middle SLOPE (90 m).

To somehow reduce influence of the meso-scale noise, we will further analyze only time series of spatial averages of D_{AW} (and other AW variables). Overall averages should provide general information on the AW layer evolution, but they may miss some local details having a genuine interannual variability as a cause. Therefore, in addition to averages over the WHOLE section, an analysis will also be made for longitudinal bands of either 1° (0.5° for some variables on the shelf) or 3° (see Fig. 1b). At 76.5°N, 1° of longitude corresponds to 26 km, which is equal to 4–5 baroclinic radii of deformation and comparable to a typical radius of eddies in the WSC area (van Aken and Budéus, 1995; Gascard et al., 1995). To further reduce the impact of non-synoptic features, the series will ultimately be smoothed also in time. Here we only note that the relative variability of D_{AW}, which is 20% for the WHOLE section (Table 1), is larger than the relative variability of θ_{AW} (10%–12%). However, both significantly contribute to the

variability of H_{AW}, so that the evolution of all 3 variables will be studied. Table 1 also shows that variations of the geostrophic transport are relatively large. The ratio of the STD and the mean V_{AW} is ~0.5 for the WHOLE section, ~1 in the SLOPE and RIDGE areas, and ~2 in the FLAT area. Similar relations are found for the heat flux because the relative variability of θ_{AW} is small. Since the evolution of F_{AW} closely follows that of V_{AW}, only the latter will be analyzed in detail.

4. Interannual variability

The eastern AW core was characterized by warmer conditions at the beginning of the 1900s and 2000s than during a short period in the second half of the 1990s (Fig. 8a–c, solid line). A warm period at the beginning of the 1990s is a feature which was identified in all time series obtained after 1980 at various locations in the NwAC/WSC system. The period was referred to as W2 by

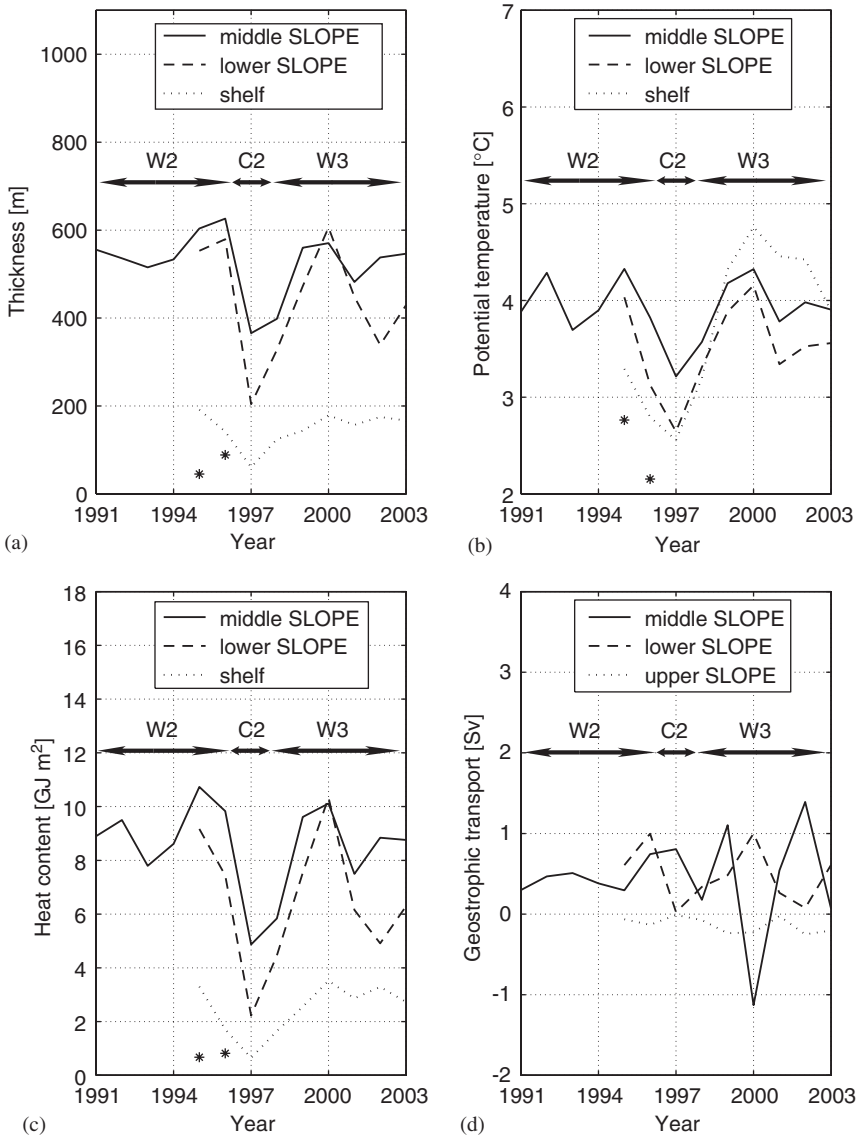

Fig. 8. Temporal development of the AW layer in the SLOPE area of the 76.5°N section: (a) Average thickness (m) on the middle (solid line) and lower (dashed line) SLOPE, and shelf area between 14.5° and 15°E (dotted line); (b) same as (a) but for average potential temperature (°C); (c) same as (a) but for average heat content (GJ m^{-2}); (d) geostrophic transport (Sv) on the middle (solid line), lower (dashed line) and upper (dotted line) SLOPE. Stars in (a)–(c) indicate values at the easternmost (15°E) station in 1995–1996. W2, C2, and W3 denote periods discussed in the text.

Furevik (2001). W2 followed a cold period in the second half of the 1980s (C1) which, on its turn, followed another warm period (W1). In the WSC, the time series of the average temperature in the 50–500 m layer at 9° and 11°E on the standard Norwegian section at 76.3°N (stations S1 and S2 in Fig. 1a), hereafter referred to as the Sørkapp series, show a sequence of cold and warm periods also before 1980 (e.g., Blindheim et al., 2000). The sequence was superimposed on a long-term trend resulting in a 1 °C warming between the mid-sixties and W2. A warming trend together with oscillatory peaks were also observed in the series of the average temperature in the 100–300 m layer on the continental slope between the 300 and 1200 m isobaths at 79–79.5°N (box NS in Fig. 1a) from 1969 to 1997 (Saloranta and Haugan, 2001), hereafter referred to as the northern slope series. The occurrence of a short, but exceptionally cold period at the beginning of the second half of the 1990s (C2), followed by a warming to 1999, was observed in the Sørkapp series (Dickson et al., 2000) and also in the θ_{AW} series obtained farther southeast, along our 15°E section (Schlichtholz and Goszczko, 2005). The passage from C2 to a warm period (W3) was further documented in a temperature series from 1997 to 2000 at 79°N (Schauer et al., 2004). A recovery to warm conditions at the end of the 1990s was also successfully modeled by hindcasts for the period 1979–1999 (Karcher et al., 2003).

At 76.5°N, the heat content in the eastern AW core showed two warm peaks during W2, in 1992 and 1995 (Fig. 8c). Similar peaks were observed in θ_{AW} on the 15°E section (Schlichtholz and Goszczko, 2005). A peak in 1992 is also seen in the northern slope series (Saloranta and Haugan, 2001, Fig. 4). However, a similar peak is absent from the Sørkapp series, in which a maximum appears 1–2 yr earlier (Dickson et al., 2000, Fig. 10). This indicates that the 1992 event was rather limited to the eastern AW core. On the other hand, a possibly concomitant occurrence of the event farther west may be masked by a different layer considered. The northern slope series were constructed for a relatively thin layer (200 m) in a relatively thick AW core while the Sørkapp series represented a relatively thick layer (450 m) in an area where the AW layer might have been relatively thin. The presence of a 1992 peak in the θ_{AW} series on the SLOPE (Fig. 8b) and its absence in the corresponding D_{AW} series (Fig. 8a) shows that the 1992 event was a shallow one.

In the north, C2 lasted from 1995 to 1998 (Schauer et al., 2004, Fig. 9). At 76.5°N, truly cold conditions in the eastern AW core were observed only for two years (1997–1998), although a cooling in an upper part of the core started already in 1996 (compare the D_{AW} and θ_{AW} series in Figs. 8a and b). This upper layer cooling was more pronounced at the edges of the core as revealed by the series on the lower SLOPE (Figs. 8a–c, dashed line) and shelf (Figs. 8a–c, dotted line). Low temperatures in 1996 were also observed farther west, in the RIDGE (Fig. 9b) and FLAT (Fig. 10b, solid line) areas. The AW layer in 1996, although not warm, was particularly thick along the entire section (Fig. 7a) except the eastern side of the Polar Front (Fig. 8a, dotted line) and the western side of the Arctic Front (Fig. 9a, dashed line). D_{AW} between these fronts in 1996 was as large as (or even larger than) in 1995, at least on the middle and lower SLOPE (Fig. 8a).

The timing of the cold peak was different in different data sets. In the northern slope series, the temperature minimum appeared as early as in 1995. However, low values of H_{AW} in 1995 were also observed on the shelf at 76.5°N (Fig. 8c, dotted line). Moreover, the interpolation might have led to a considerable overestimation of temperature on the shelf in 1995 when a station on the eastern side of the Polar Front, at 14.5°E, was missing. The AW layer at the easternmost station in 1995 was as cold as in 1996 (stars in Figs. 8a–c). This suggests that the 1995 minimum in the northern slope series might have been related to stations in shallower water. In the Sørkapp series, which represent conditions on the eastern side of the Knipovich Ridge, a temperature minimum appeared in 1996. A slightly lower temperature in 1996 than in 1997, when averaged over the same layer as in the Sørkapp series, was also found in the western RIDGE area at 76.5°N (not shown). Therefore, an eddy or a local displacement of the Arctic Front might be an explanation for a different timing of the cold peak in the two datasets. The minimum in 1997 is a robust feature, seen in θ_{AW} and D_{AW} all along the 76.5°N section (Figs. 8a–b, 9a–b and 10a–b) and also in θ_{AW} along the 15°E section (Schlichtholz and Goszczko, 2005).

Our data suggest that W3 has recently declined. This is most evident in the evolution of the overall H_{AW} in which a decreasing trend was established after 2000 (Fig. 10c, dashed line). Nearly a half of the heat gain between 1997 and 2000, which was equivalent to a surface heat flux of $\sim$40 W m^{-2}, was

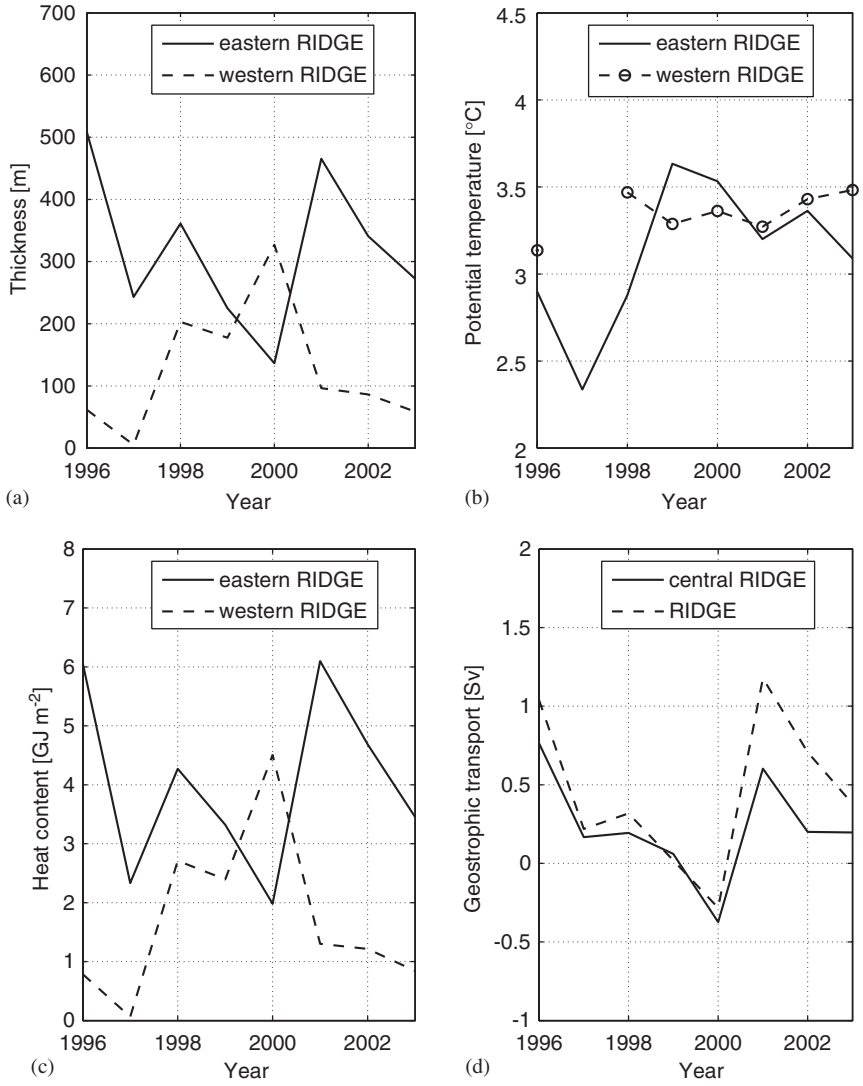

Fig. 9. Temporal development of the AW layer in the RIDGE area of the 76.5°N section: (a) Average thickness (m) in the eastern (solid line) and western (dashed line) RIDGE area; (b) same as (a) but for average potential temperature (°C); (c) same as (a) but for average heat content (GJ m^{-2}); (d) geostrophic transport (Sv) in the central (solid line) and entire (dashed line) RIDGE area.

lost from 2000 to 2003. These are huge quantities, comparable to the annual mean surface heat flux of 35–47 W m^{-2} in the Norwegian Sea (Simonsen and Haugan, 1996). After a cooling in 2001, a secondary overall warming occurred in 2002, but it was a shallow one since it is seen only in θ_{AW} (Fig. 10b, dashed line) and not in D_{AW} (Fig. 10a, dashed line). The overall D_{AW} showed a bi-annual maximum in 2000–2001 which was retarded by 1 yr compared to a bi-annual peak of the overall θ_{AW}. The warm event in 2002, which occurred in the FLAT area (Fig. 10b, solid line) as well as in the RIDGE and SLOPE areas (Figs. 9b and 8b) was perhaps related to a change in the circulation regime. V_{AW} on the lower and upper SLOPE evolved in phase till, but not after 2001 (Fig. 8d).

A particular evolution of the AW layer occurred in the eastern RIDGE area where a minimum (in 2000) and a maximum (in 2001) of D_{AW} and H_{AW} occurred in opposite phase to the corresponding peaks on the middle SLOPE (compare solid lines in Figs. 9a and c with solid lines in Figs. 8a and c). A negative correlation between the temperature (100–400 m average) in the western and eastern branches of the NwAC has been reported by Mork and Blindheim (2000) on the basis of hydrographic

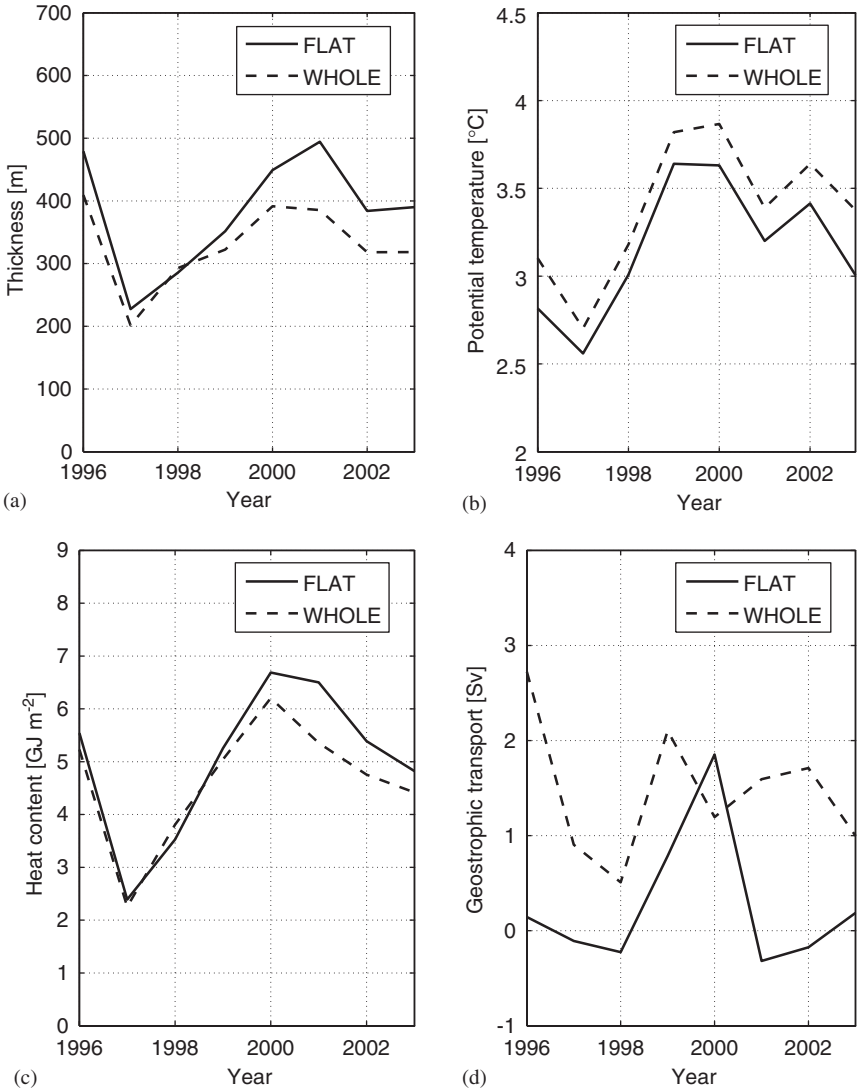

Fig. 10. Temporal development of the AW layer in the FLAT area (solid lines) and the WHOLE 76.5°N section (dashed lines): (a) Average thickness (m); (b) average potential temperature (°C); (c) average heat content (GJ m^{-2}); (d) geostrophic transport (Sv).

measurements from 1978 to 1996 on the Svinøy section (Fig. 1a). However, at 76.5°N, the presence of an extremely thick AW layer in 1996 was concomitant in both AW cores. We have found a more robust relationship between D_{AW} (and H_{AW}) on the opposite sides of the RIDGE area where the major extremes were negatively correlated (Figs. 9a and c). Such a correlation is in accordance with the evolution of V_{AW} in the central RIDGE area which achieved a minimum (southward flow) in 2000 and maxima in 1996 and 2001 (Fig. 9d, solid line). In 2001, when the Arctic Front was strong and broad (Fig. 7b), the transport in the entire RIDGE area reached a value of 1.2 Sv, which was even slightly larger than the corresponding value in 1996 (Fig. 9d, dashed line), when the Arctic Front was strong and narrow.

5. Correlations with the NAO index

The NAO index, based on the normalized difference of the sea level pressures at Lisbon (Portugal) and Stykkisholmur (Iceland), is available back to 1864 (Hurrel, 1995). Correlations (r) of the winter (December–March mean) values of the index with some AW variables on the 76.5°N section are given in Table 2 where also correlations (r_s) for smoothed (3-yr running mean) series are included.

Table 2
Correlations of chosen AW variables (symbols explained in Section 2) in different areas of the 76.5°N section (Fig. 1b) with the winter NAO index. Lag 0 (1) refers to the correlation with the NAO index for the same (previous) calendar year. Correlations r and r_s are for the unsmoothed data and the 3-yr running mean values, respectively. The series were detrended before correlation. Values in parentheses (underlined) are significant at the 95% (99%) level. The number of degrees of freedom (NDF) for the unsmoothed series is equal to $N-2$ (N—number of years). NDF for the smoothed series (NDF_s) is estimated by the method of Davis (1976).

Variable	Area	Period	Lag	r	r_s	NDF_s
θ_{AW}	Middle SLOPE	1991–2003	0	0.53	0.74	3.5
θ_{AW}	Middle SLOPE	1991–2003	1	0.44	(0.86)	3.6
D_{AW}	Middle SLOPE	1991–2003	1	(0.70)	(0.96)	3.6
H_{AW}	Middle SLOPE	1991–2003	1	(0.61)	(0.96)	3.7
V_{AW}	Lower SLOPE	1995–2003	1	(0.77)	(0.90)	3.0
θ_{AW}	WHOLE	1996–2003	0	0.51	0.88	1.9
θ_{AW}	WHOLE	1996–2003	1	0.39	0.63	3.4
D_{AW}	WHOLE	1996–2003	1	(0.94)	(0.96)	2.6
H_{AW}	WHOLE	1996–2003	1	(0.83)	0.89	2.8
V_{AW}	WHOLE	1996–2003	1	0.56	0.80	2.4
V_{AW}	WHOLE	1996–2003	0	−0.46	−0.26	5.6
D_{AW}	Western RIDGE	1996–2003	0	0.68	0.90	2.0
D_{AW}	Eastern RIDGE	1996–2003	0	(−0.89)	(−0.99)	2.0
V_{AW}	Central RIDGE	1996–2003	0	(−0.96)	(−0.99)	2.0

Smoothing reduces the number of degrees of freedom which, for the smoothed series (NDF_s), has been calculated using an autocorrelation method (Davis, 1976).

A comparison of the evolution of the NAO index and θ_{AW} on the middle SLOPE shows a good qualitative agreement between the series (Fig. 11a). The warm period in the first half of the 1990s and the peak in θ_{AW} at the turn of the century had their equivalents in high values of the NAO index while the short cold period in between is reminiscent of the extreme negative value of the NAO index in 1996. Even a decreasing tendency at the beginning of the 2000s is a common feature of both series. Moreover, the timing of all maxima in the NAO index (1992, 1995, 2000 and 2002) and two from the three minima (1993 and 2001) exactly fits the timing of the corresponding extremes in θ_{AW}. However, the major temperature minimum (in 1997) appeared 1 yr after the NAO negative extreme, and an extremely low temperature persisted for an additional year. Consequently, the correlation between the 1991–2003 series is not high ($r=0.53$) and significant only at a low level (between 90% and 95%). This conclusion is not changed when the smoothed series are considered ($r_s=0.74$). The

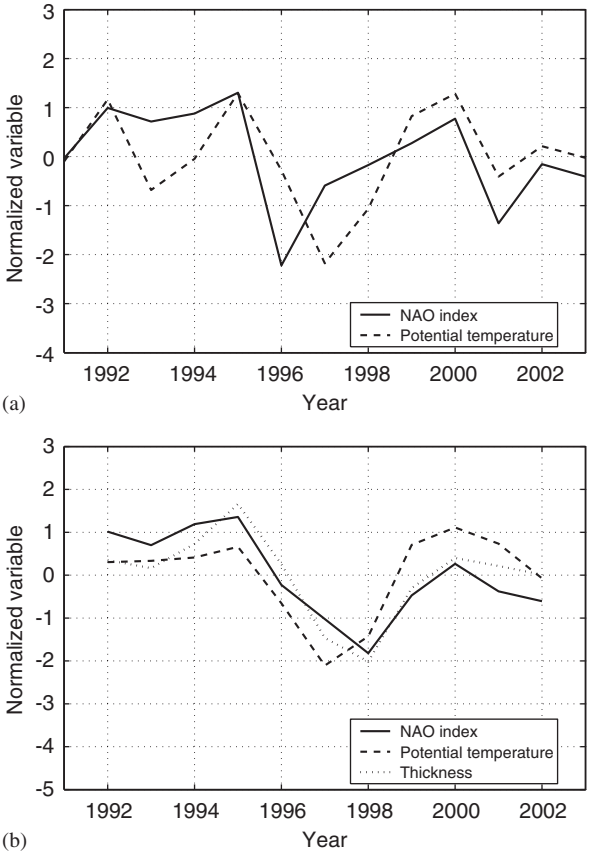

Fig. 11. Temporal development of the NAO index and average properties of the AW layer in the middle SLOPE area of the 76.5°N section in the 1991–2003 period. All variables are normalized by subtracting the means and dividing by the standard deviations in that period: (a) NAO index (solid line) and AW temperature (dashed line); (b) 3-yr running means of the NAO index (solid line), AW temperature (dashed line) and AW layer thickness (dotted line). In (b), the NAO index is shifted 1 yr forward to better illustrate a retardation of the AW properties.

smoothed series reveal even better than the unsmoothed series that θ_{AW} (Fig. 11b, dashed line) had a tendency to be retarded with respect to the NAO index (Fig. 11b, solid line). The correlation between the smoothed θ_{AW} series (1992–2002) and the 1-yr shifted smoothed NAO index (1991–2001) is significant at the 95% level ($r_s=0.86$). The correlation with the shifted NAO index is even higher in the case of D_{AW} (Fig. 11b, dotted line) or H_{AW}. For both smoothed variables, the correlation ($r_s=0.96$) is significant at the 99% level. The lagged correlation is relatively high even in the case of the unsmoothed D_{AW} series.

The retardation of D_{AW} with respect to the NAO index becomes even more pronounced if we consider

the AW layer on the WHOLE section. Fig. 12a shows a good fit between the development of the overall D_{AW} in the 1996–2003 period and the shifted NAO index (1995–2002). Even though the series are not smoothed, the correlation is very high ($r = 0.94$). This is because not only the layer thinning after the major NAO index drop in 1996, but also the layer thinning after the second abrupt index drop in 2001 was retarded by 1 yr. The correlation for the overall H_{AW} is lower ($r = 0.83$) but still significant at the 95% level. A lower correlation for H_{AW} is due to the contribution from

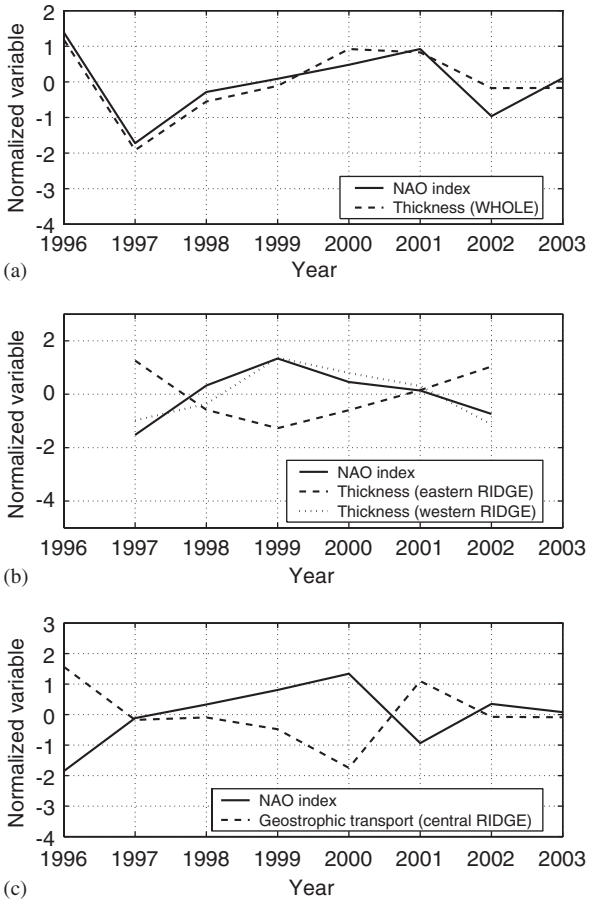

Fig. 12. Temporal development of the NAO index and AW properties in different areas of the 76.5°N section in the 1996–2003 period. All variables are normalized for that period: (a) NAO index (solid line) and average AW thickness in the WHOLE section (dashed line). The NAO index is shifted 1 yr forward to better illustrate a retardation of the AW layer thickness; (b) 3-yr running means of the NAO index (solid line) and average AW thickness in the eastern (dashed line) and western (dotted line) RIDGE area; (c) NAO index (solid line) and geostrophic transport in the central RIDGE area (dashed line).

θ_{AW} which, as in the AW core alone, is better correlated with the NAO index in the no-lag case than in the lag case. A difference between the SLOPE and WHOLE areas is that the smoothing of θ_{AW} in the latter increased the correlation in the non-lag case ($r_s = 0.88$) more than in the lag case.

There is a local exception from the general rule that D_{AW} lags the NAO index. In the secondary AW core area, D_{AW} changed in tune with, but in opposite phase to the NAO index. The correlation between the non-lagged series is high for either the smoothed data ($r_s = -0.99$, Fig. 12b, solid and dashed lines) or the unsmoothed data ($r = -0.89$). The smoothed D_{AW} series in the eastern RIDGE area shows an opposite-phase evolution also when compared to the corresponding series in the western RIDGE area (Fig. 12b, dotted line), a feature already noted for the major extremes in the unsmoothed series (Fig. 9a). In the case of the western RIDGE area, the correlation of the D_{AW} series with the NAO index is however lower ($r_s = 0.90$) than in the case of the eastern RIDGE area.

The opposite-phase evolution of D_{AW} on the opposite sides of the RIDGE area together with their non-lagged correlations with the NAO index suggest that a major direct effect of the NAO on the WSC should be seen in the evolution of the geostrophic flow in the western branch of the current. Indeed, the (negative) correlation between the NAO index and V_{AW} in the central RIDGE area is extremely high even for the unsmoothed series ($r = -0.96$, Fig. 12c). An equally high correlation ($r = -0.94$) is obtained for V_{AW} in the entire RIDGE area (Fig. 9d, dashed line). The high values of the transport in 1996 and 2001 were associated with the low values of the NAO index while the high value of the NAO index in 2000 was concomitant with the reversal of the flow direction. Also the eastern branch of the WSC responded to the NAO changes, but the response was rather retarded. Indeed, the 1995–2003 series of V_{AW} on the lower SLOPE (Fig. 8d, dashed line) are significantly correlated (at the 95% level) only with the shifted NAO index (1994–2002). The correlation is positive and lower ($r = 0.77$) than in the case of the western branch. The lower correlation is mainly a result of the maximum transport on the lower SLOPE in 2000.

The most evident links to the NAO, i.e., a lagged response of the overall D_{AW}, which mostly represents the variability in the FLAT area between the

eastern and western branches (Fig. 10a), and a non-lagged response of V_{AW} in the western branch seem to be verified upstream of the WSC, at least during W3. The evolution of the overall D_{AW} in the NwAC on the MRN section, which mostly runs over a flat area north of the Lofotan Basin (Fig. 1a), closely follows the evolution of D_{AW} in the FLAT area on the 76.5°N section from 2000 to 2003 (Fig. 13a). Similarly, the evolution of V_{AW} on the Mohns Ridge slope corresponds to the evolution of V_{AW} in the trench of the Knipovich Ridge (Fig. 13b).

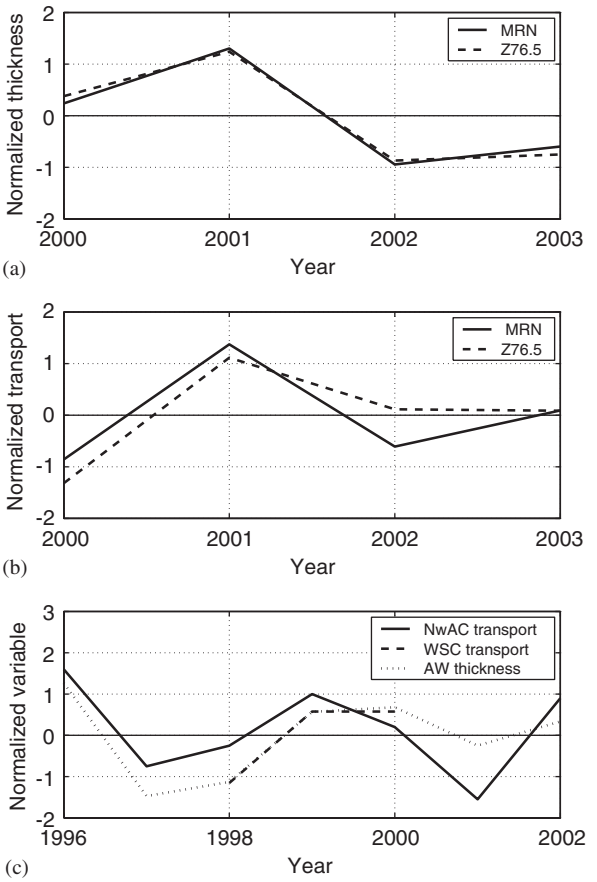

Fig. 13. Comparison of the evolution of normalized AW variables on different sections (see Fig. 1a): (a) Layer thickness averaged over the MRN section (solid line) and the FLAT area of the 76.5°N section (dashed line); (b) geostrophic transport across the western part of the MRN section (solid line) and the central RIDGE area of the 76.5°N section (dashed line); (c) annual mean transport in the eastern branch of NwAC on the Svinøy section (solid line), based on current measurements (Orvik and Skagseth, 2003, Fig. 4), and in the WSC at 79°N (dashed line), also based on current measurements (Schauer et al., 2004, Fig. 8), and the layer thickness in the middle SLOPE area of the 76.5°N section (dotted line). In (a), (b), the minimum and maximum values of the layer thickness (geostrophic transport) on the MRN section correspond to 560 and 590 m (2.3 and 4.7 Sv). In (c), the annual mean values of the transport for both the NwAC and the WSC are winter centered so that a value plotted, e.g., for 1999 corresponds to the mean from summer 1998 to 1999. The extreme values for the NwAC (WSC) correspond to 3.3 and 5 Sv (3.1 and 4 Sv).

6. Discussion with concluding remarks

6.1. Transport estimates

Our transport estimates at 76.5°N (Table 1) are small compared to the estimates based on the ADCP-referenced geostrophic flow obtained using the same hydrographic data. For instance, Piechura et al. (2002) reported a net transport of AW ($\theta > 2\,^{\circ}C, S > 34.92$) across the 76.5°N section in 2000 equal to 5.8 Sv and the associated heat flux of 100 TW. The large differences between our and the ADCP-referenced estimates cannot be attributed to strong interannual variability since the baroclinic transport in 2000 is representative for the mean (Fig. 10d, dashed line). The differences can only partly be caused by a different assumption on the near-bottom velocity shear between station pairs with uneven bottom depth or to a more westward extension of the 76.5°N section in the ADCP-referenced calculations. Major differences result from a depth-independent component of flow which, in the ADCP-measurements, could include a noise related to the sea level gradients caused by high-frequency atmospheric perturbations. A barotropic along-slope flow in the WSC can also be maintained by a time-mean remote forcing via the continuity requirement or by local along-isobath density gradients as is the case in the EGC (Schlichtholz and Houssais, 1999c; Schlichtholz, 2002, 2005). A strong depth-independent flow in the eastern branch of the NwAC/WSC is documented by long-term current meter measurements upstream (Orvik et al., 2001; Skagseth et al., 2004) as well as downstream (Fahrbach et al., 2001; Schauer et al., 2004) of the 76.5°N section. However, the depth-independent flow, if averaged over a sufficiently long period, may not be large in summer. For instance, the monthly mean values of fluxes in Fram Strait estimated from the current meter data at 79°N show a strong annual cycle. The northward volume (heat) flux in the AW ($\theta > 1\,^{\circ}C$) layer in 1999 dropped from ~10 Sv (~80 TW) in February to ~3 Sv (~35 TW) in August (Schauer et al., 2004, Fig. 4). The summer minima are comparable to the northward baroclinic fluxes in the AW

layer across our 76.5°N section in 1999 (2.4 Sv and 45 TW).

Summer hydrographic data on the Svinøy section in the 1978–1996 period show that the baroclinic transport of AW ($\theta > 1\,^{\circ}C$) is larger in the western branch (nearly two-thirds of the overall baroclinic transport across the section) than in the eastern branch (Mork and Blindheim, 2000). Similarly, more than a half of the overall AW transport across our MRN section, which amounts to 5.8 ± 1.1 Sv, is associated with the western branch (3.3 ± 1.0 Sv). An estimate of the baroclinic transport of AW (hydrographic data from May 2000, level of no motion at 700 m depth) across a zonal section at 74.5°N (Z74.5 in Fig. 1a) is 2.5 Sv (Gascard et al., 2004). This value is close to our estimate of the mean overall transport in the 0–1000 db layer at 76.5°N in the 1996–2003 period (2.1 Sv) and falls within the range of variations in the AW transport (Fig. 10d). In contrast to the estimates for the NwAC, a larger contribution to the baroclinic transport of AW in the WSC comes from the eastern branch (Table 1). However, this is an effect of a reduced layer thickness in the RIDGE area, which still contributes a half (1 Sv) to the overall transport in the 0–1000 db layer. The hydrographic data on the Svinøy section also indicate a compensating tendency of the two branches with regard to both long-term trends and interannual variability in the baroclinic transport (Mork and Blindheim, 2000). This is not observed in the WSC at 76.5°N in the 1996–2003 period. The discrepancy may result not only from different periods of measurements, but also from the fact that the NwAC is partly diverted towards the Barents Sea.

Skagseth et al. (2004) demonstrated, using current meter data from the eastern (mostly barotropic) branch on the Svinøy section and some altimeter data in the 1995–2002 period that variations of the along-slope flow on time scales from 1 to 12 months are likely to be coherent from the Irish–Scottish shelf to Fram Strait. Orvik and Skagseth (2003) showed, using the same current meter data, a significant variability of the 1-yr moving means of the AW ($S > 35$) transport series, from which yearly (winter centered) values are reproduced here in Fig. 13c (solid line). For the WSC at 79°N, Schauer et al. (2004) reported an increase of the annual mean transport of AW over the continental slope (from the shelf break to the 2400 m isobath) by ~1 Sv from 1997–1998 to 1998–1999 (Fig. 13c, dashed line). The increase corresponds to a similar but slightly smaller increase of the Svinøy transport. Although a depth-independent component is missed in our flow series, its influence may be reflected in variations of water properties at 76.5°N as shown by comparison of variations in the strength of the NwAC/WSC with the evolution of the eastern AW core thickness (Fig. 13c, dotted line) and the baroclinic transport at the edges of the core (Fig. 8d). A good correspondence of the curves in Fig. 13c suggests that summer changes of D_{AW} may be used as an indicator of the variability in the annual mean volume transport in the WSC. Advection of D_{AW} by a flow anomaly may be a mechanism responsible for this link. Because of a northward decrease of temperature in the WSC (Saloranta and Haugan, 2004), a positive (negative) flow anomaly should increase (decrease) D_{AW}. A transport anomaly of 1 Sv corresponds to a velocity anomaly of $1\,cm\,s^{-1}$ for an area of $100\,km^2$. Such an anomaly should induce a year to year change of D_{AW} by 150 m, as observed on the middle SLOPE at 76.5°N between 1998 and 1999 (Fig. 8a), for an along-stream gradient of D_{AW} equal to 50 m per 100 km.

6.2. Competition between a lagged and non-lagged response to the NAO

Links of variability in the Nordic Seas area and the NAO may vary from period to period, perhaps in relation to changes in the position of the NAO's centers (e.g., Dickson et al., 2000). One of the questions is whether the temperature in the WSC, when correlated, lags the NAO index or not. The first estimate, based on the measurements on the Sørkapp section in the period 1978–1993, indicated that the summer temperature (50–200 m average) was correlated ($r = 0.6$) but lagged the winter NAO index (Swift et al., 1997). However, a subsequent analysis of the Sørkapp series in the period 1967–1996 revealed a no-lag correlation ($r_s = 0.8$) between the temperature (50–500 m average) and the NAO index (Blindheim et al., 2000; Dickson et al., 2000). A problem with establishing a clear lag was also reported for the northern slope series (Saloranta and Haugan, 2001). The correlation for the autumn temperature was low in the period 1970–1994, with the highest value in the no-lag case ($r_s = 0.4$). However, when the period 1970–1974 was excluded from the analysis, the correlation increased for different time lags, with the highest value ($r_s = 0.85$) in the case of a 1-yr lag.

A tendency to lag the NAO index was also shown by the summer AW temperature on our 15°E section in the 1991–1999 period (Schlichtholz and Goszczko, 2005). However, the highest correlation ($r_s = 0.93$) was found in the no-lag case.

The lag problem emerges also on the 76.5°N section. We have shown that while the eastern AW core temperature rather lags the NAO index (Fig. 11b), the overall θ_{AW} is better correlated with the NAO index in the no-lag case (Table 2). However, this conclusion, as most of the inferences for the temperature in the WSC described above, is based on the 3-yr running mean series. The unsmoothed series in the eastern core area show, apart from the mismatch in 1996–1997, a concomitance of all extremes in the 1991–2003 period (Fig. 11a). If this is not a coincidence, our data demonstrate a change of regime from an 'immediate' response to the NAO during W2 to a lagged response during C2, and a return to an 'immediate' response during W3.

A competition between a lagged and non-lagged response also concerns the vertical structure of temperature evolution as revealed by comparison of the AW temperature and thickness series. In contrast to the overall θ_{AW}, the overall D_{AW} is highly correlated and lags the NAO index by 1 yr (Fig. 12a). A lagged response is also evident in the eastern core area alone (Fig. 11b) where, however, the drop of the NAO index in 2001 left an 'immediate' imprint on D_{AW} (Fig. 8a). Some vertical dependence of the lag between the NAO index and temperature during W2 was also evidenced from a low-passed-filtered series in the Barents Sea opening (Furevik, 2001).

A competition between a lagged and non-lagged response is most evident in the cross-section structure of the AW thickness evolution. In contrast to the SLOPE and FLAT areas, D_{AW} in the RIDGE area is correlated with the non-lagged NAO index. While the correlation for the western RIDGE area is positive, the correlation for the eastern RIDGE area is negative (Fig. 12b), so that the transport in the western branch of the WSC is negatively correlated with the NAO index (Fig. 12c). A negative correlation of AW properties (depth of the 3 °C isotherm, average temperature in the 100–400 m layer, and the 1st EOF for temperature in the 50–800 m layer) with the NAO index was also reported for a western core in the NwAC from an analysis of the summer data on the Svinøy section from 1978 to 1996 (Mork and Blindheim, 2000). These data show a moderate positive correlation for the overall (baroclinic) transport of AW. There is also a positive, but lagged and non-significant correlation for the overall AW transport across the 76.5°N section (Table 2).

6.3. Mechanisms of the link with the NAO

Mechanisms shaping relations between the evolution of the AW layer on the 76.5°N section and the NAO are multiple. For instance, advection of layer properties by flow anomalies may be linked to the NAO-related forcing through a flow variability which is coherent along the continental slope off Scotland to Fram Strait. Such a response is suggested by a good agreement of the thickness of the eastern AW core in the WSC and the annual mean AW transport in the eastern branch of the NwAC on the Svinøy section (Fig. 13c). The 1-yr moving means of the Svinøy transport are correlated with the basin-wide average wind stress curl at 55°N 15 months earlier (Orvik and Skagseth, 2003). Orvik and Skagseth (2003) interpreted the delayed signal in the Svinøy transport in the framework of Sverdrup dynamics as an along-slope barotropic response on a baroclinic time scale in the northern North Atlantic. Our results point to a baroclinic manifestation of that response in the WSC.

The second mechanism is related to a more immediate response manifested in a weakening (strengthening) of the Arctic Front with the increase (decrease) of the NAO index which enhances (prohibits) exchanges across the front. The comparison of the AW transport along the Mohns and Knipovich ridges (Fig. 13b) shows that even though the anomalous transport in the RIDGE area at 76.5°N in 2000 might be a result of a local instability, the associated eddying should be linked with a regional weakening of the front. Similarly, the maximum strength of the western branch at 76.5°N in 2001 is an effect of a regional strengthening of the front. The western branch was particularly strong also after the spectacular drop of the NAO index in 1996, as seen from our data at 76.5°N (Fig. 9d) and a 5 Sv increase of the baroclinic transport of AW across the western part of the Svinøy section from spring 1995 to 1996 (Mork and Blindheim, 2000, Fig. 14). A similar increase was not observed in the summer data, most likely because of a westward shift of the front as indicated by a nearly 200 m deepening of the AW layer over the same part of the section (Mork and Blindheim, 2000, Fig. 12).

The changes of the strength of the Arctic Front are likely to be affected by winds over the Nordic Seas. An increased (decreased) cyclonicity of the wind stress in the area corresponds to periods of a positive (negative) NAO index (Karcher et al., 2003; Jakobsen et al., 2003). This may affect the Arctic Front in the following manner. In years with a high NAO index the northeasterly winds over the EGC strengthen (e.g., Dickson et al., 2000, Fig. 2). As a consequence, the East Greenland Polar Front sharpens, so that the PW layer is squeezed against the Greenland coast and not allowed to enter the Greenland gyre. This leaves room for AW and increases exchanges across the Arctic Front. On the other hand, a drop of the NAO is associated with a weakening and more northerly direction of winds over the EGC. The East Greenland Polar Front weakens and PW invades the Greenland gyre, so that the Arctic Front sharpens because its position is kept fixed by the Mohns and Knipovich ridges. A decreased (increased) thickness of the western core of AW in the NwAC/WSC during a high (low) NAO index seems also to be in accordance with stronger (weaker) westerly winds into the Nordic Seas which tend to squeeze (relax) the AW layer against the Norwegian coast and increase (decrease) its transport towards the Barents Sea.

A mechanism contributing to a correlation between the heat content anomalies in the WSC and the NAO is the heat exchange with the atmosphere during the northward flow of AW through the Nordic Seas. During periods with a positive (negative) NAO index more (less) warm air is advected by the stronger (weaker) westerlies into the Nordic Seas area which reduces (increases) the local winter heat loss to the atmosphere. Temperature anomalies created in this way are then advected by the NwAC towards Fram Strait. This mechanism was first proposed by Swift et al. (1997) to explain the lag between their temperature series in the WSC and the NAO index. The major cold event at 76.5°N in 1997 (Figs. 10a–c) is consistent with a large positive (more heat loss to the atmosphere) annual mean (July 1996 to June 1997 average) heat flux anomaly over the NwAC area (Karcher et al., 2003, Fig. 11). Similarly, the warming of the AW layer during subsequent years has a counterpart in a significant reduction and then reversal of the sign of the surface heat flux anomaly. Karcher et al. (2003) also show that positive heat content anomalies during W2 could have been created by an increased inflow of AW across the GSR. This is in contrast to findings of Furevik (2001) who attributed the temperature increase in this period to variations in atmospheric heat fluxes. However, Furevik (2001) considered only changes in the 50–200 m layer.

Temperature anomalies may also be advected to Fram Strait from the northern North Atlantic. A northward passage of temperature anomalies created outside the Nordic Seas was reported by Furevik (2001) for the W1 and C1 cases. A particularly strong, deep reaching (below the depth of the gaps in the GSR) temperature anomaly was observed by Bersch et al. (1999) along a summer hydrographic section between Greenland and Ireland (WOCE in Fig. 1a). While there was a rather gradual increase of the thickness of the warm and saline Subpolar Mode Water upstream of the eastern branch of the NwAC from 1991 to 1996, the thickness of this water mass upstream of the western branch peaked in 1996. Bersch et al. (1999) linked the peak to the advection from the subtropics on one hand and, on the other hand, to a local reduction of the Ekman upwelling and the ocean-to-atmosphere heat flux in the subpolar gyre in response to the NAO drop in 1996. A possible advective signature of this anomaly in Fram Strait can be seen in the AW thickness peak in 2000–2001 (Fig. 10a). A 4–5 yr lag would require an advective velocity of $3-4\,\mathrm{cm\,s^{-1}}$.

It is worth emphasizing that the 1996 anomaly south of the GSR was concomitant with the deepening of the AW layer on the western side of the Svinøy section and an extremely thick western AW core on the 76.5°N section (Fig. 9a). This points to coherent, NAO-forced changes along the Subarctic and Arctic fronts down to Fram Strait. It would be interesting to see whether such coordinated changes are limited to extreme events or are a more general rule. A high correlation with the NAO in the WSC suggests that the latter may be true, at least from 1996 onwards.

Acknowledgements

The authors acknowledge the National Center for Atmospheric Research (NCAR), U.S., for providing the NAO index data via anonymous ftp. Computational support was provided by the Academic Computer Center in Gdansk TASK. I.G. has been funded by the Arctic–Subarctic Ocean Fluxes (ASOF) project of EC under Framework Programme 5.

References

Aagaard, K., Swift, J.H., Carmack, E.C., 1985. Thermohaline circulation in the Arctic Mediterranean Seas. Journal of Geophysical Research 90 (C5), 4833–4846.

Bersch, M., Meincke, J., Sy, A., 1999. Interannual thermohaline changes in the northern North Atlantic 1991–1996. Deep-Sea Research, Part II 46, 55–75.

Blindheim, J., Borovkov, V., Hansen, B., Malmberg, S.-A., Turrell, W.R., Østerhus, S., 2000. Upper layer cooling and freshening in the Norwegian Sea in the relation to atmospheric forcing. Deep-Sea Research, Part I 47, 655–680.

Davis, R.E., 1976. Predictability of sea surface temperature and sea level pressure anomalies over the North Pacific Ocean. Journal of Physics and Oceanography 6, 249–266.

Dickson, R.R., Osborn, T.J., Hurrell, J.W., Meincke, J., Blindheim, J., Adlandsvik, B., Vinje, T., Alekseev, G., Maslowski, W., 2000. The Arctic Ocean response to the North Atlantic Oscillation. Journal of Climate 13, 2671–2696.

Fahrbach, E., Meincke, J., Østerhus, S., Rohardt, G., Schauer, U., Tverberg, V., Verduin, J., 2001. Direct measurements of volume transports through Fram Strait. Polar Research 20, 217–224.

Furevik, T., 2001. Annual and interannual variability of Atlantic Water temperatures in the Norwegian and Barents Seas. Deep-Sea Research, Part I 48, 383–404.

Gascard, J.-C., Richez, C., Rouault, C., 1995. New insights on large-scale oceanography in Fram Strait: The West Spitsbergen Current. Coastal and Estuarine Studies Series American Geophysics Union, New York, pp. 131–182.

Gascard, J.-C., Watson, A.J., Messias, M.-J., Johannessen, K.A.O., Simonsen, T., 2002. Long-lived vortices as a mode of deep ventilation in the Greenland Sea. Nature 416 (6880), 525–527.

Gascard, J.-C., Raisbeck, G., Sequeira, S., Yiou, F., Mork, K.A., 2004. The Norwegian Atlantic Current in the Lofoten basin inferred from hydrological and tracer data (^{129}I) and its interaction with the Norwegian Coastal Current. Geophysical Research Letters 31, L01308.

Hurrel, J.W., 1995. Decadal trends in the North Atlantic Oscillation: regional temperature and precipitation. Science 269, 676–679.

Jakobsen, P.K., Ribergaard, M.H., Quadfasel, D., Schmith, T., Hughes, C.W., 2003. Near-surface circulation in the northern North Atlantic as inferred from Lagrangian drifters: variability from mesoscale to interannual. Journal of Geophysical Research 108 (C8), 3251.

Karcher, M.J., Gerdes, R., Kauker, F., Koberle, C., 2003. Arctic warming: evolution and spreading of the 1990s warm event in the Nordic seas and the Arctic Ocean. Journal of Geophysical Research 108 (C2), 3034.

Mauritzen, C., 1996. Production of dense overflow waters feeding the North Atlantic across the Greenland-Scotland Ridge. Part 1: Evidence of a revised circulation scheme. Deep-Sea Research, Part I 43, 769–806.

Morgan, P., 1994. SEAWATER: A library of MATLAB computational routines for the properties of sea water. Report 222, CSIRO Marine Laboratories.

Mork, K.A., Blindheim, J., 2000. Variations in the Atlantic inflow to the Nordic Seas, 1955–1996. Deep-Sea Research, Part I 47, 1035–1057.

Orvik, K.A., Niiler, P., 2002. Major pathways of Atlantic water in the northern North Atlantic and Nordic Seas toward Arctic. Geophysical Research Letters 29 (19), 1896.

Orvik, K.A., Skagseth, Ø., 2003. The impact of the wind stress curl in the North Atlantic on the Atlantic inflow to the Norwegian Sea toward the Arctic. Geophysical Research Letters 31 (17), 1884.

Orvik, K.A., Skagseth, Ø., Mork, M., 2001. Atlantic inflow to the Nordic Seas: current structure and volume fluxes from moored current meters, VM-ADCP and SeaSoar-CTD observations, 1995–1999. Deep-Sea Research, Part I 48, 937–957.

Piechura, J., Osinski, R., Petelski, T., Wozniak, S.B., 2002. Heat and salt fluxes in the West Spitsbergen Current area in summer. Oceanologia 44 (3), 307–321.

Saloranta, T.M., Haugan, P.M., 2001. Interannual variability in the hydrography of Atlantic water northwest of Svalbard. Journal of Geophysical Research 106 (C7), 13931–13943.

Saloranta, T.M., Haugan, P.M., 2004. Northward cooling and freshening of the warm core of the West Spitsbergen Current. Polar Research 23 (1), 79–88.

Saloranta, T.M., Svendsen, H., 2001. Across the Arctic front west of Spitsbergen: high-resolution CTD sections from 1998–2000. Polar Research 20 (2), 177–184.

Schauer, U., Fahrbach, E., Østerhus, S., Rohardt, G., 2004. Arctic warming through Fram Strait: Oceanic heat transport from 3 years of measurements. Journal of Geophysical Research 109, C06026.

Schlichtholz, P., 2002. On a modified arrested topographic wave in Fram Strait. Journal of Geophysical Research 107 (C11), 3189.

Schlichtholz, P., 2005. Climatological baroclinic forcing of the barotropic flow in the East Greenland Current in Fram Strait. Journal of Geophysical Research 110, C08013.

Schlichtholz, P., Goszczko, I., 2005. Was the Atlantic Water temperature in the West Spitsbergen Current predictable in the 1990s? Geophysical Research Letters 32, L04610.

Schlichtholz, P., Houssais, M.-N., 1999a. An inverse modeling study in Fram Strait. Part I: dynamics and circulation. Deep-Sea Research, Part II 46, 1083–1135.

Schlichtholz, P., Houssais, M.-N., 1999b. An inverse modeling study in Fram Strait. Part II: water mass distribution and transports. Deep-Sea Research, Part II 46, 1137–1168.

Schlichtholz, P., Houssais, M.-N., 1999c. An investigation of the dynamics of the East Greenland Current in Fram Strait based on a simple analytical model. Journal of Physics and Oceanography 29, 2240–2265.

Schlichtholz, P., Houssais, M.-N., 2002. An overview of the $\theta - S$ correlations in Fram Strait based on the mizex 84 data. Oceanologia 44 (2), 243–272.

Schlichtholz, P., Jankowski, A., 1993. Hydrological regime and water volume transport in the Faeroe-Shetland Channel in summer of 1988 and 1989. Oceanological Acta 16, 11–22.

Simonsen, K., Haugan, P.M., 1996. Heat budgets of the Arctic Mediterranean and sea surface heat flux parameterizations for the Nordic Seas. Journal of Geophysical Research 101 (C3), 6553–6576.

Skagseth, Ø., Orvik, K.A., 2002. Identifying fluctuations in the Norwegian Atlantic Slope Current by means of empirical orthogonal functions. Continental Shelf Research 22, 547–563.

Skagseth, Ø., Orvik, K.A., Furevik, T., 2004. Coherent variability of the Norwegian Atlantic Slope Current derived from TOPEX/ERS altimeter data. Geophysical Research Letters 31, L14304.

Swift, J.H., Aagaard, K., Carmack, E.C., Hingston, M., Macdonald, R.W., McLaughlin, F.A., Perkin, R.G., 1997. Waters of the Makarov and Canada basins. Deep-Sea Research, Part II 44, 1503–1529.

van Aken, H.M., Budéus, G., 1995. The anatomy of the Arctic Frontal Zone in the Greenland Sea. Journal of Geophysical Research 100 (C8), 15999–16014.